

# Insight into Hadron Structure from Lattice QCD

J.W. Negele

Center for Theoretical Physics

Laboratory for Nuclear Science and Department of Physics  
Massachusetts Institute of Technology, Cambridge MA 02139  
MIT-CTP # 2676 hep-lat/9709129

March 24, 2024

## Abstract

A variety of evidence from lattice QCD is presented revealing the dominant role of instantons in the propagation of light quarks in the QCD vacuum and in light hadron structure. The instanton content of lattice gluon configurations is extracted, and observables calculated from the instantons alone are shown to agree well with those calculated using all gluons. The lowest 128 eigenfunctions of the Dirac operator are calculated and shown to exhibit zero modes localized at the instantons. Finally, the zero mode contributions to the quark propagator alone are shown to account for essentially the full strength of the  $\rho$  and pion resonances in the vector and pseudoscalar correlation functions.

## Introduction

For the nearly three decades since the experimental discovery of quarks and the formulation of QCD, understanding the essential physics of light quarks in QCD and the structure of light hadrons has remained an elusive goal. Since analytic theoretical techniques are as yet inadequate to solve QCD, a number of very different QCD-inspired models have been developed that present quite disparate physical pictures. For example, non-relativistic quark models focus on constituent quarks interacting via an adiabatic potential. Bag models postulate a region in which relativistic current quarks are confined and interact by gluon exchange. Motivated by large  $N_c$  arguments, Skyrme models describe the nucleon as a topological soliton built out of qq pairs. Finally instanton models emphasize the role of topological structures in the vacuum corresponding in the

---

This work is supported in part by funds provided by the US Department of Energy (DOE) under cooperative research agreement # DF-FC 02-94ER 40818.

semiclassical limit to instantons and of the quark zero modes associated with these topological excitations.

How can one understand which, if any, of these fundamentally different pictures describes the essential physics of light hadrons? Phenomenology has proven inconclusive, with each of the models being rich enough that with sufficient embellishment it can be made to fit the data. Whereas perturbative QCD has proven extremely useful in extracting quark and gluon structure functions from high energy scattering experiments, it is inadequate to understand their origin. Hence, it is necessary to turn to nonperturbative methods, and the only known techniques to solve, rather than model QCD, is lattice field theory. Our strategy, then, will be to use the fact that lattice calculations numerically evaluate the path integral for QCD as a tool to identify the paths that dominate the path integral and thereby identify the physics that dominates hadron structure.

The lattice results described below indicate that gluons play an extremely important dynamical role in light hadrons. Thus, QCD with light quarks is unique among the many-body systems with which we are familiar in the sense that the quanta generating the interactions cannot be subsumed into a potential but rather participate as essential dynamical degrees of freedom. In atoms, for example, photons play a negligible dynamical role, and to an excellent approximation may be subsumed into the static Coulomb potential. In nuclei, mesons play a minor dynamical role, and to a good approximation nuclear structure may be described in terms of two- and three-body nucleon forces. Indeed, experimentalists need to work very hard and pick their cases carefully to observe any effects of meson exchange currents. And in heavy quark systems, much of the physics of  $c\bar{c}$  and  $b\bar{b}$  bound states may be understood by subsuming the gluons into an adiabatic potential with Coulombic and confining behavior. It turns out that nucleons, however, are completely different in that gluons are crucial dynamical degrees of freedom. This result is not entirely unexpected, since from perturbative QCD, we already know by the work of Gross and Wilczek [1] and Hoodbhoy, Ji and Tang [2] that approximately half ( $16=3n_f$  to be precise, where  $n_f$  is the number of active flavors and equals 5 below the top quark mass) of the momentum and angular momentum comes from glue in the limit of high  $Q^2$ . Furthermore, experiment tells us that this behavior continues down to non-perturbative scales of the order of several  $\text{GeV}^2$ .

The physical picture that arises from this work corresponds closely to the physical arguments and instanton models of Shuryak and others [3, 4, 5] in which the zero modes associated with instantons produce localized quark states, and quark propagation proceeds primarily by hopping between these states. The support that lattice calculations provide for this picture includes quantitative determination of the instanton content of the QCD vacuum, a comparison of the effects of all gluon contributions versus those of instantons alone, direct calculation of the quark zero modes, and demonstration that these modes dominate the rho and pion contributions to vector and pseudoscalar correlation functions.

## Background

### Lattice QCD

A QCD observable is evaluated by defining quark and gluon variables on the sites and links of a space-time lattice, writing a Euclidean path integral of the generic form [6]

$$\begin{aligned} \langle H \rangle e^{-B_H} &= \int \prod U D(U) e^{-M(U) - S(U)} \\ &= \int \prod U D(U) e^{\ln \det M(U) - S(U)} M^{-1}(U) M^{-1}(U) \end{aligned} \quad (1)$$

and evaluating the final integral over gluon link variables  $U$  using the Monte Carlo method. The link variable is  $U = e^{iagA(x)}$ , the Wilson gluon action is  $S(U) = \frac{2N}{g^2} \sum_t (1 - \frac{1}{N} \text{ReTr} U_t)$  where  $U_t$  denotes the product of link variables around a single plaquette, and  $M(U)$  denotes the discrete Wilson approximation to the inverse propagator  $M(U) = m + \not{D} + i g A$ . Evolution in Euclidean time is required to assure a dominantly positive integral and thus to obtain a statistically accurate Monte Carlo result, and we will utilize the fact that the Euclidean evolution operator projects out the lowest energy state having a specified set of quantum numbers:

$$e^{-B_H} = \sum_n e^{-B_{E_n}} C_n = \sum_n e^{-B_{(E_1, E_0)}} C_n \quad (2)$$

A physical way of understanding the final integral in (1) is to expand  $M^{-1}(1 + u)^{-1}$  in powers of the so-called hopping parameter which couples neighboring sites with gauge fields, and thereby generate all the quark time-histories. In the case of propagation of a meson from  $x$  to  $y$ , the integral for  $\langle H \rangle e^{-B_H}(y)(y)(x)(x)$  has the following three contributions. Expansion of the two  $M^{-1}(U)$  terms generates all valence quark and antiquark trajectories that begin at the source  $x$  and terminate at the sink  $y$ . Expansion of  $\ln \det M(U)$  generates all disconnected quark loops corresponding to excitation of quark-antiquark pairs from the Dirac Sea. Omission of the determinant, which is very expensive computationally, yields the so-called quenched approximation in which the quark-antiquark pairs excited from the sea are neglected. Finally, when the sum over all plaquettes in  $S(U)$  is expanded out of the exponent, the lattice is tiled in all possible ways by any number of plaquettes. After integration over  $\prod U$ , only those combinations of link variables from expanding  $M^{-1}(U)$  and  $S(U)$  survive that correspond to color singlets. The simplest non-vanishing tiling for a meson corresponds to completely tiling the region between the valence quark and antiquark with gluon plaquettes. If one imagines cutting this and more and more complicated tilings on a single time slice, one obtains the physical picture of a quark and antiquark (from cutting the two valence quark lines generated by  $M^{-1}$ ) connected by a gluon flux tube (from cutting all the gluon surfaces that connect the quark and antiquark).

Typical lattices range from  $16^3 \times 32$  to  $32^3 \times 64$  and thus involve numerical integrations over  $10^7$  to  $10^8$  real variables.

## Correlation functions

As in the case of other strongly interacting many-body systems, to understand the structure of the vacuum and light hadrons in nonperturbative QCD, it is instructive to study appropriately selected ground state correlation functions, to calculate their properties quantitatively, and to understand their behavior physically.

The vacuum correlation functions we consider are the point-to-point equal time correlation functions of hadronic currents

$$R(x) = \langle T J(x) J(0) \rangle \quad (3)$$

discussed in detail by Shuryak [3] and recently calculated in quenched lattice QCD [7]. The motivation for supplementing knowledge of hadron bound state properties by these correlation functions is clear if one considers the deuteron. Simply knowing the binding energy, mass radius, quadrupole moment and other ground state properties yields very little information about the nucleon-nucleon interaction in each spin, isospin and angular momentum channel as a function of spatial separation. To understand the nuclear interaction in detail, one inevitably would be led to study nucleon-nucleon scattering phase shifts. Although, regrettably, our experimental colleagues have been most inept in providing us with quark-antiquark phase shifts, the same physical information is contained in the vacuum hadron current correlation functions  $R(x)$ . As shown by Shuryak [3], in many channels these correlators may be determined or significantly constrained from experimental data using dispersion relations. Since numerical calculations on the lattice agree with empirical results where available, we regard the lattice results as valid solutions of QCD in all channels and thus use them to obtain information comparable to scattering phase shifts.

The correlation functions we calculate in the pseudoscalar, vector, nucleon and Delta channels are

$$\begin{aligned} R(x) &= \langle T J^P(x) J^P(0) \rangle ; \\ R(x) &= \langle T J(x) J(0) \rangle ; \\ R(x) &= \frac{1}{4} \text{Tr} \langle T J^N(x) J^N(0) \rangle_{ix} ; \end{aligned}$$

and

$$R(x) = \frac{1}{4} \text{Tr} \langle T J(x) J(0) \rangle_{ix} ;$$

where

$$\begin{aligned} J^P &= u_5 d ; \\ J &= u_5 d ; \\ J^N &= \frac{1}{\sqrt{3}} [u^a C u^b]_5 d^c ; \end{aligned}$$

and

$$J = \epsilon_{abc} [u^a C u^b] u^c :$$

As in Refs. [3] and [7], we consider the ratio of the correlation function in QCD to the correlation function for non-interacting massless quarks,  $R(x) = R_0(x)$ , which approaches one as  $x \rightarrow 0$  and displays a broad range of non-perturbative effects for  $x$  of the order of 1 fm. Typical results of lattice calculations of ratios of vacuum correlation functions are shown in Fig. 1.

Note that the lattice results (solid line) agree well with phenomenological

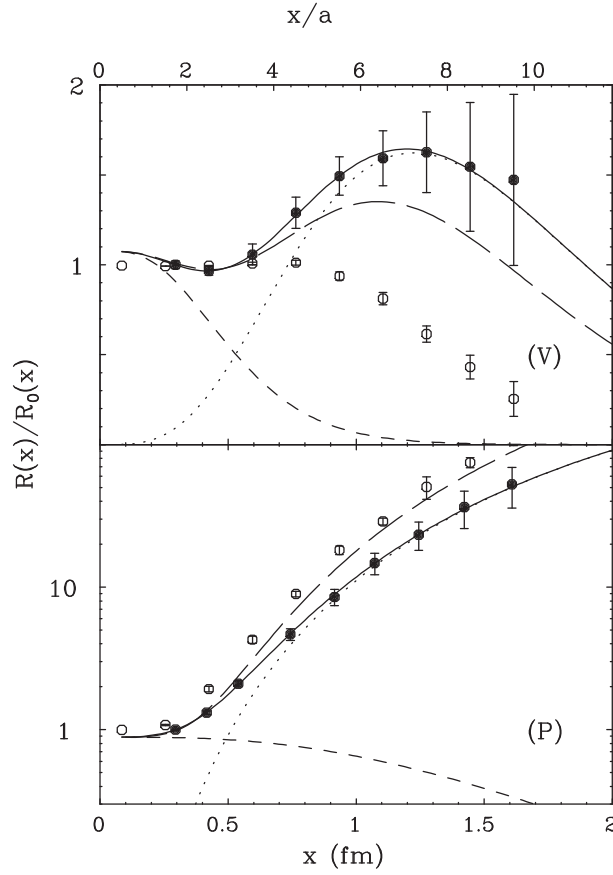


Figure 1: Vector (V) and Pseudoscalar (P) correlation functions are shown in the upper and lower panels respectively. Lattice results [7] are denoted by the solid points with error bars and by the solid curves, which may be decomposed into continuum and resonance components denoted by short dashed and dotted curves respectively. Phenomenological results determined by dispersion analysis of experimental data in Ref. [3] are shown by long dashed curves, and the open circles denote the results of the random instanton model of Ref. [4].

results from dispersion analysis of data (long dashed curves). Also, observe that the vector and pseudoscalar correlation functions are strongly dominated by the rho and pion contributions (dotted lines) in the region of 0.5 to 1.5 fm. We will subsequently show that these rho and pion contributions in turn arise from the zero mode contributions associated with instantons.

As discussed in Refs. [3, 7], these vacuum correlators show strong indications of instanton dominated physics. As shown by 't Hooft [8], the instanton induced interaction couples quarks and antiquarks of opposite chirality leading to strong attractive and repulsive forces in the pseudoscalar and scalar channels respectively and no interaction to leading order in the vector channel. Just this qualitative behavior is observed at short distance in all the channels we computed. Furthermore, as shown by the open circles with error bars in Fig. 1, the random instanton model of Shuryak et al. [4] reproduces the main features of the correlation functions at large distance as well.

## Instantons

The QCD vacuum is understood as a superposition of an infinite number of states of different winding number, where the winding number characterizes the number of times the group manifold is covered when one covers the physical space. Just as there is a stationary point in the action of the Euclidean Feynman path integral for a double well potential corresponding to the tunneling between the two degenerate minima, so also there is a classical solution to the QCD equations in Euclidean time, known as an instanton [9], which describes tunneling between two vacuum states of differing winding number. The action associated with an instanton is

$$S_0 = \frac{1}{4} \int d^4x F^a_{\mu\nu} F^{\mu\nu a} = \frac{48}{g^2} \int d^4x \frac{1}{x^2 + \frac{1}{2}}^4 = \frac{8\pi^2}{g^2} : \quad (4)$$

Note that the action density has a universal shape characterized by a size  $\rho$ , and that the action is independent of  $\rho$ . Furthermore, the instanton field strength is self-dual, i.e.  $F^a_{\mu\nu} = \tilde{F}^a_{\mu\nu} = \frac{1}{2} \epsilon_{\mu\nu\alpha\beta} F^{\alpha\beta a}$ , so that the topological charge of an instanton is

$$Q = \frac{g^2}{8\pi^2} \int d^4x F^a_{\mu\nu} \tilde{F}^{\mu\nu a} = 1 :$$

Two features of instantons are particularly relevant to light hadron physics. The first is the fact that although the fermion spectrum is identical at each minimum of the vacuum, quarks of opposite chirality are raised or lowered one level between adjacent minima. Thus, an instanton absorbs a left-handed quark of each flavor and emits a right-handed quark of each flavor, and an anti-instanton absorbs right-handed quarks and emits left-handed quarks. Omitting heavier quarks for simplicity, the resulting 't Hooft interaction involving the operator  $u_R u_L d_R d_L s_R s_L$  is the natural mechanism to describe otherwise puzzling aspects of light hadrons. It is the natural mechanism to flip the helicity of a valence quark and transmit this helicity to the glue and quark-antiquark pairs, thereby

explaining the so-called "spin crisis." It also explains why the two valence u quarks in the proton would induce twice as many  $\bar{d}d$  pairs as the  $u\bar{u}$  pairs induced by the single valence d quark. The second feature is that each instanton gives rise to a localized zero mode of the Dirac operator  $D_0(x) = 0$ . Hence, considering a spectral representation of the quark propagator, it is natural that the propagator for the light quarks is dominated by these zero modes at low energy. This gives rise to a physical picture in which  $q\bar{q}$  pairs propagate by "hopping" between localized modes associated with instantons.

## Instanton Content of Lattice Gluon Configurations

### Identifying instantons by cooling

The Feynman path integral for a quantum mechanical problem with degenerate minima is dominated by paths that fluctuate around stationary solutions to the classical Euclidean action connecting these minima [10]. In the case of the double well potential, a typical Feynman path is composed of segments fluctuating around the left and right minima joined by segments crossing the barrier. If one had such a trajectory as an initial condition, one could find the nearest stationary solution to the classical action numerically by using an iterative local relaxation algorithm. In this method, which has come to be known as cooling, one sequentially minimizes the action locally as a function of the coordinate on each time slice and iteratively approaches a stationary solution. In the case of the double well, the trajectory approaches straight lines in the two minima joined by kinks and antikinks crossing the barrier and the structure of the trajectory can be characterized by the number and positions of the kinks and antikinks.

In QCD, the corresponding classical stationary solutions to the Euclidean action for the gauge field connecting degenerate minima of the vacuum are instantons, and we apply the analogous cooling technique [11] to identify the instantons corresponding to each gauge field configuration.

The results of using 25 cooling steps as a filter to extract the instanton content of a typical gluon configuration are shown in Fig. 2, taken from Ref. [12] using the Wilson action on a  $16^3 \times 24$  lattice at  $\beta = g^2 = 5.7$ . As one can see, there is no recognizable structure before cooling. Large, short wavelength fluctuations of the order of the lattice spacing dominate both the action and topological charge density. After 25 cooling steps, three instantons and two anti-instantons can be identified clearly. The action density peaks are completely correlated in position and shape with the topological charge density peaks for instantons and with the topological charge density valleys for anti-instantons. Note that both the action and topological charge densities are reduced by more than two orders of magnitude so that the fluctuations removed by cooling are several orders of magnitude larger than the topological excitations that are retained.

Setting the coupling constant, or equivalently, the lattice spacing, and quark

mass by the nucleon and pion masses in the usual way, it turns out that the characteristic size of the instantons identified by cooling is  $0.36 \text{ fm}$  and the density is  $1.6 \text{ fm}^{-4}$ , in reasonable agreement with the value of  $0.33 \text{ fm}$  and  $1.0 \text{ fm}^{-4}$  in the liquid instanton model[4].

### Comparison of results with all gluons and with only instantons

One dramatic indication of the role of instantons in light hadrons is to compare observables calculated using all gluon contributions with those obtained using

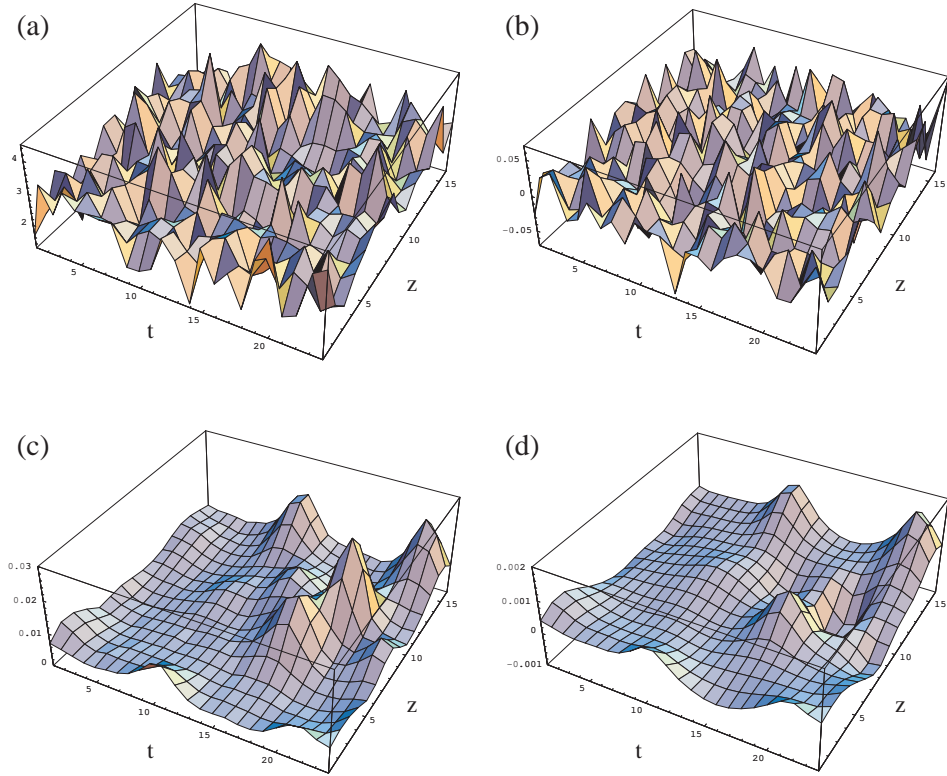


Figure 2: Instanton content of a typical slice of a gluon configuration at fixed  $x$  and  $y$  as a function of  $z$  and  $t$ . The left column shows the action density  $S(1;1;z;t)$  before cooling (a) and after cooling for 25 steps (c). The right column shows the topological charge density  $Q(1;1;z;t)$  before cooling (b) and after cooling for 25 steps.

only the instantons remaining after cooling. Note that there are truly dramatic differences in the gluon content before and after cooling. Not only has the action density decreased by two orders of magnitude, but also the string tension has decreased to 27% of its original value and the Coulombic and magnetic hyperfine components of the quark-quark potential are essentially zero. Hence, for example, the energies and wave functions of charmed and B mesons would be drastically changed.

As shown in Fig. 3, however, the properties of the rho meson are virtually unchanged. The vacuum correlation function in the rho (vector) channel and the spatial distribution of the quarks in the rho ground state, given by the ground state density-density correlation function [13]  $\langle \bar{q}_0 q(x) q_0 q(0) \rangle$ , are statistically indistinguishable before and after cooling. Also, as shown in Ref. [11], the rho mass is unchanged within its 10% statistical error. In addition, the pseudoscalar, nucleon, and delta vacuum correlation functions and nucleon and pion density-density correlation functions are also qualitatively unchanged after cooling, except for the removal of the small Coulomb induced cusp at the origin of the pion.

Although these cooling studies strongly indicate that instantons play an essential role in light quark physics, cooling has the disadvantage of modifying the instanton content of the original gluon configuration. It is possible to avoid the gradual shrinkage of a single instanton until it eventually falls through the lattice by using an improved action that is sufficiently scale independent [14]. However, pairs of instantons and anti-instantons will eventually attract each other and annihilate, thereby continually eroding the original distribution. Hence, it is valuable to complement these cooling calculations by studies of the zero modes associated with instantons, which, as we show in the next section, can be carried out successfully on the original uncooled gluon configurations.

## Quark Zero Modes and Their Contributions to Light Hadrons

### Eigenmodes of the Dirac operator

In the continuum limit, the Dirac operator for Wilson fermions approaches the familiar continuum result

$$D_x = \gamma_\mu \frac{1}{2} (\nabla_\mu + \nabla_\mu^*) u_x; \quad \nabla_\mu u_x = \frac{1}{a} [u(x+a\hat{\mu}) - u(x-a\hat{\mu})]; \quad \nabla_\mu^* u_x = \frac{1}{a} [u(x-a\hat{\mu}) - u(x+a\hat{\mu})] : \quad (1)$$

In the free case, the continuum spectrum is  $\frac{1}{m} [m + i\hat{p}]$  and the Wilson lattice operator approximates this spectrum in the physical regime and pushes the unphysical fermion modes to very large (real) masses. In the presence of an instanton of size  $\rho$  at  $x = 0$ , it is shown in Ref. [15] that the lattice operator

produces a mode with zero imaginary part that approaches the continuum result

$$\rho_0(x)_S = u_S; \frac{p^2}{(x^2 + 2)^{3/2}}$$

and whose mixing with other modes goes to zero as the lattice volume goes to infinity. In addition, instanton-anti-instanton pairs that interact sufficiently

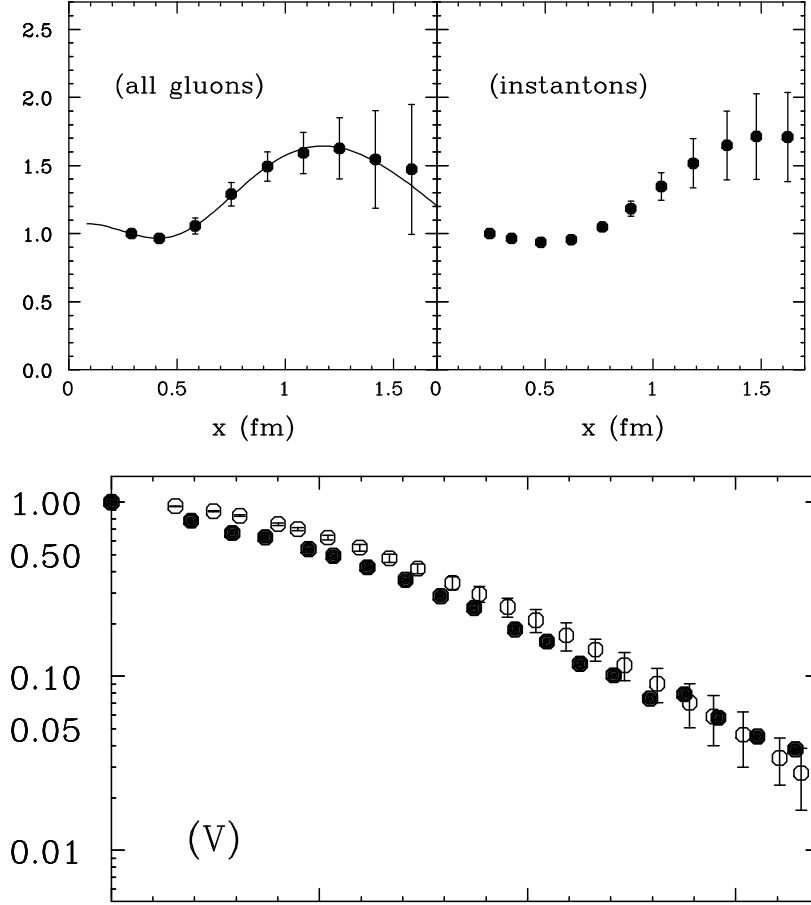


Figure 3: Comparison of  $\rho$  observables calculated with allgluon configurations and only instantons. The upper left-hand plot shows the vacuum correlator in the  $\rho$  channel calculated with allgluons as in Fig. 1 and the upper right-hand plot shows the analogous result with only instantons. The lower plot shows the ground state density-density correlation function for the  $\rho$  with allgluons (solid circles) and with only instantons (open circles). Error bars for the solid circles are comparable to the open circles and have been suppressed for clarity.

form complex conjugate pairs of eigenvalues that move slightly off the real axis. Thus, by observing the Dirac spectrum for a lattice gluon configuration containing a collection of instantons and anti-instantons, it is possible to identify zero modes directly in the spectrum.

Fig. 4 shows the lowest 64 complex eigenvalues of the Dirac operator on a  $16^4$  unquenched gluon configuration for  $6=g^2 = 5.5$  and  $\beta = 0.16$ , both before and after cooling (where 100 relaxation steps with a parallel algorithm are comparable to 25 cooling steps). The lower, cooled, plot has just the structure we expect with a number of isolated instantons with modes on the real axis and pairs of interacting instantons slightly off the real axis. However, even though the uncooled case shown in the upper plot also contains fluctuations several orders of magnitude larger than the instantons (as seen in Fig. 2), it shows the same structure of isolated instantons and interacting pairs. To set the scale, note that if we had antiperiodic boundary conditions in time, the lowest Matsubara mode ( $ip = i\frac{\pi}{T}$ ) would occur at 0.06 on the imaginary axis, so all the modes below this value are presumably the results of zero modes.

### Zero mode expansion

The Wilson Dirac operator has the property that  $D = \gamma_5 D^\dagger \gamma_5$ , which implies that  $\langle j | \gamma_5 | i \rangle = 0$  unless  $i = j$  and we may write the spectral representation of the propagator

$$\langle x | D^{-1} | y \rangle = \sum_i \frac{\langle x | \gamma_5 | i \rangle \langle i | \gamma_5 | y \rangle}{h_i} \quad (1)$$

where  $i = \gamma_i$ . A clear indication of the role of zero modes in light hadron observables is the degree to which truncation of the expansion to the zero mode zone reproduces the result with the complete propagator.

Fig. 5 shows the result of truncating the vacuum correlation functions for the vector and pseudoscalar channels to include only low eigenmodes [15]. On a  $16^4$  lattice, the full propagator contains 786,432 modes. The top plot of Fig. 5 shows the result of including the lowest 16, 32, 64, 96, and finally 128 modes. Note that the first 64 modes reproduce most of the strength in the rho resonance peak pointed out in Fig. 1, and by the time we include the first 128 modes, all the strength is accounted for. Similarly, the lower plot in Fig. 5 shows that the lowest 128 modes also account for the analogous pion contribution to the pseudoscalar vacuum correlation function. Thus, without having to resort to cooling, by looking directly at the contribution the lowest eigenfunctions, we have shown that the zero modes associated with instantons dominate the propagation of rho and pions in the QCD vacuum.

### Localization

Finally, it is interesting to ask whether the lattice zero mode eigenfunctions are localized on instantons. This was studied by plotting the quark density distribution for individual eigenmodes in the x-z plane for all values of y and t,

and comparing with analogous plots of the action density. As expected, for a cooled configuration the eigenmodes correspond to linear combinations of localized zero modes at each of the instantons. (Because there are no symmetries, the coefficients are much more complicated than the even and odd combinations in a double well or the Bloch waves in a periodic potential.) What is truly remarkable, however, is that the eigenfunctions of the uncooled configurations also exhibit localized peaks at locations at which instantons are identified by cooling. Thus, in spite of the fluctuations several orders of magnitude larger than the instanton fields themselves, the light quarks essentially average out these fluctuations and produce localized peaks at the topological excitations. When one analyzes a number of eigenfunctions, one finds that all the instantons remaining after cooling correspond to localized quark fermion peaks in some eigenfunctions. However, some fermion peaks are present for the initial gluon configurations that do not correspond to instantons that survive cooling. These presumably correspond to instanton-anti-instanton pairs that were annihilated during cooling.

## Conclusion

Altogether, the lattice calculations reported here provide strong evidence that instantons play a dominant role in quark propagation in the vacuum and in light hadron structure. We have shown that the instanton content of gluon configurations can be extracted by cooling, and that the instanton size and density is consistent with the instanton liquid model. We obtain striking agreement between vacuum correlation functions, ground state density-density correlation functions, and masses calculated with all gluons and with only instantons. Zero modes associated with instantons are clearly evident in the Dirac spectrum, and account for the  $\rho$  and  $\pi$  contributions to vector and pseudoscalar vacuum correlation functions. Finally, we have observed directly quark localization at instantons in uncooled configurations.

## Acknowledgments

It is a pleasure to acknowledge the essential role of Richard Brower, Ming Chu, Je-Grandy, Suzhou Huang, Taras Ivananko, Kostas Orginos, and Andrew Pochinsky who collaborated in various aspects of this work. We are also grateful for the donation by Sun Microsystems of the 24 Gops E5000 SMP cluster on which the most recent calculations were performed and the computer resources provided by NERSC with which this work was begun.

## References

- [1] Gross D., and Wilczek F., Phys. Rev. D 9, 980 (1974).
- [2] Ji X., Tang J., and Hoodbhoy P., Phys. Rev. Lett. 76, 740 (1996).

- [3] Shuryak E.V., Rev. Mod. Phys. 65, 1 (1993), Nucl. Phys. B (Proc. Suppl.) 34, 107 (1994), and Schaerer T., and Shuryak E.V., hep-ph/9610451v2.
- [4] Shuryak E.V., and Verbaarschot J.J.M., Nucl. Phys. B 410, 55 (1993); Schaerer T., Shuryak E.V., and Verbaarschot J.J.M., Nucl. Phys. B 412, 143 (1994).
- [5] Dyakanov D.I., and Petrov V.Yu, Nucl. Phys. B 245, 259 (1984); B 272, 457 (1986).
- [6] See for example, Creutz M., Quarks, Gluons and Lattices, Cambridge: Cambridge Univ. Pr., 1983.
- [7] Chu M.-C., G Randy J.M., Huang S., and Negele J.W., Phys. Rev. Lett. 70, 225 (1993); Phys. Rev. D 48, 3340 (1993).
- [8] 't Hooft G., Phys. Rev. D 14, 3432 (1976).
- [9] Belavin A.A., Polyakov A.M., Schwartz A.P., and Tyupkin Y.S. Phys. Lett. 59B, 85 (1975).
- [10] Negele J.W., and Orland H., Quantum Many-Particle Systems, New York: Addison-Wesley, 1987.
- [11] Berg B., Phys. Lett. 104B, 475 (1981); Teper M., Nucl. Phys. B (Proc. Suppl.) 20, 159 (1991).
- [12] Chu M.-C., G Randy J.M., Huang S., and Negele J.W., Phys. Rev. D 49, 6039 (1994).
- [13] Chu M.-C., Lissia M., and Negele J.N., Nucl. Phys. B 360, 31 (1991); Lissia M., Chu M.-C., Negele J.W., and G Randy J.M., Nucl. Phys. A 555, 272 (1993).
- [14] de Forcrand P., Garcia Perez M., and Stamatescu I.O., hep-lat/9701012 (1997).
- [15] Ivanenko T., M II Ph.D. dissertation 1997; Ivanenko T., and Negele J.W., Proceedings of Lattice '97, to be published.

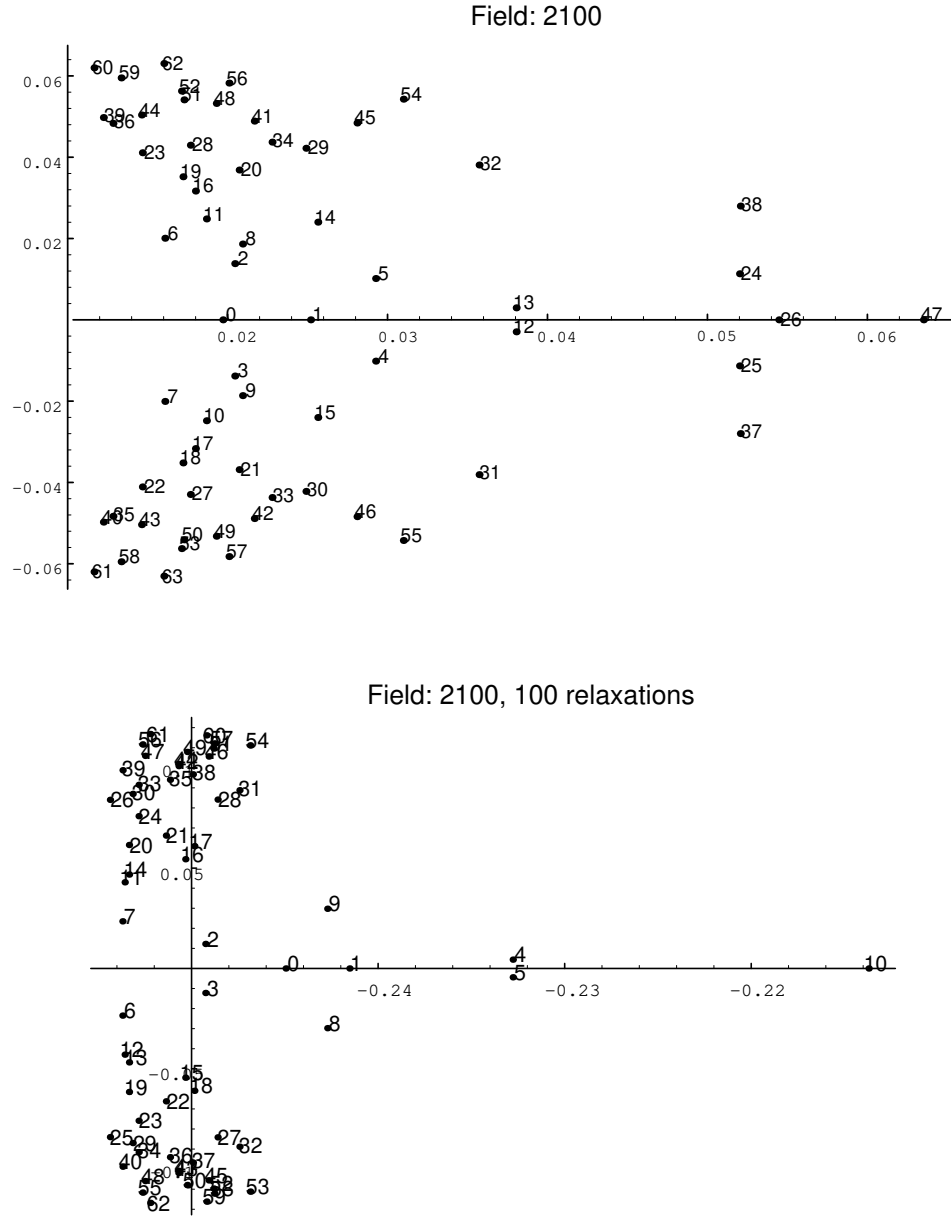


Figure 4: Lowest 64 complex eigenvalues of the Wilson-Dirac operator for an unquenched gluon configuration both before (upper plot) and after cooling (lower plot). The scale is such that 0.06 on the imaginary axis roughly corresponds to the lowest Matsubara frequency, 380 MeV.

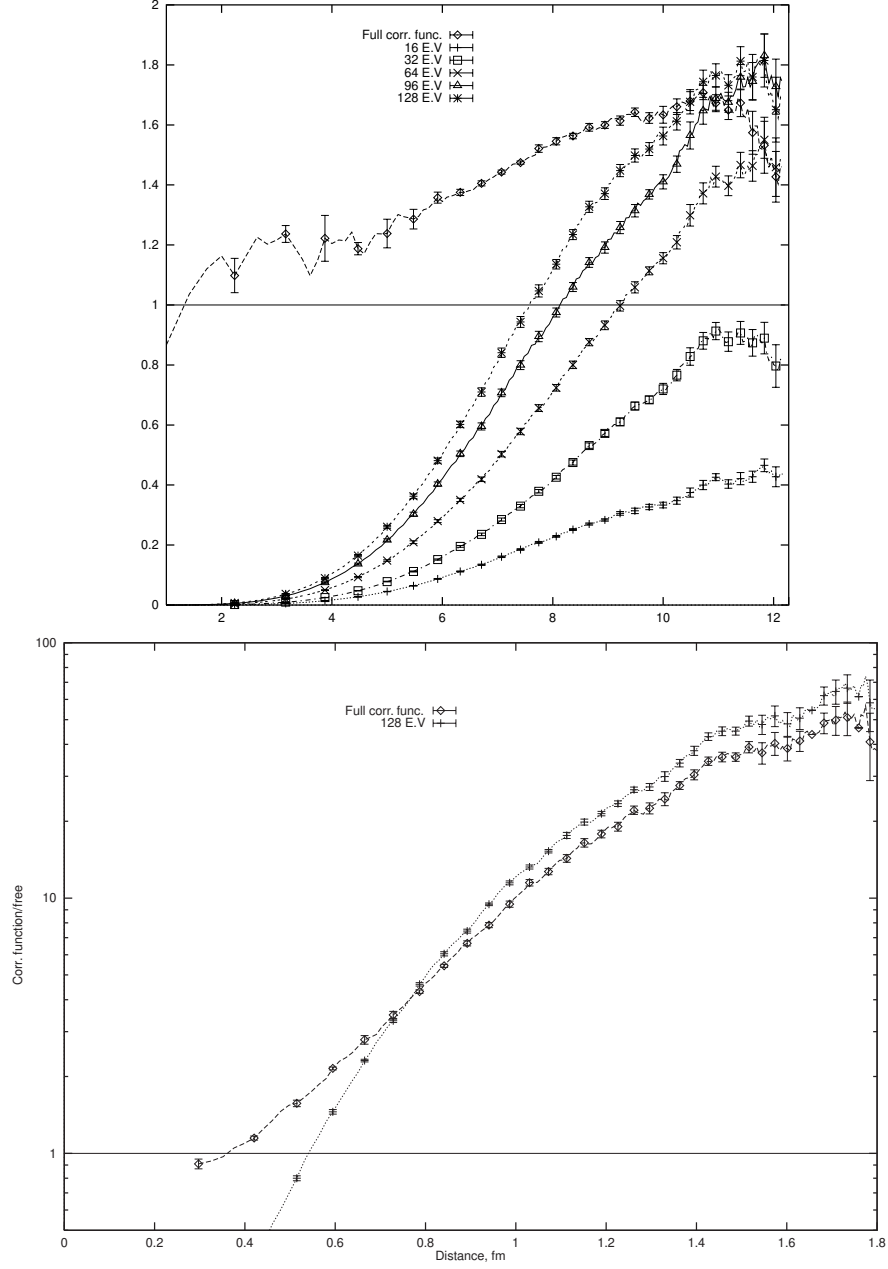


Figure 5: Contributions of low Dirac eigenmodes to the vector (upper graph) and pseudoscalar (lower graph) vacuum correlation functions. The upper graph shows the contributions of 16, 32, 64, 96, and 128 eigenmodes compared with the full correlation function for an unquenched configuration with a 63 MeV valence quark mass. The lower graph compares 128 eigenmodes with the full correlation function for a quenched configuration with a 23 MeV quark mass.